

# Unveiling carbon dimers and their chains as precursor of graphene growth on Ru(0001)

Cite as: Appl. Phys. Lett. **109**, 131604 (2016); <https://doi.org/10.1063/1.4963283>

Submitted: 20 July 2016 . Accepted: 11 September 2016 . Published Online: 28 September 2016

Min Gao, Yan-Fang Zhang, Li Huang, Yi Pan, Yeliang Wang, Feng Ding, Yuan Lin, Shi-Xuan Du, and Hong-Jun Gao



View Online



Export Citation



CrossMark

## ARTICLES YOU MAY BE INTERESTED IN

[Communication: Stable carbon nanoarches in the initial stages of epitaxial growth of graphene on Cu\(111\)](#)

The Journal of Chemical Physics **134**, 171105 (2011); <https://doi.org/10.1063/1.3587239>

[Edge states of graphene wrinkles in single-layer graphene grown on Ni\(111\)](#)

Applied Physics Letters **109**, 143103 (2016); <https://doi.org/10.1063/1.4963858>

[Quasi-free-standing graphene nano-islands on Ag\(110\), grown from solid carbon source](#)

Applied Physics Letters **110**, 213107 (2017); <https://doi.org/10.1063/1.4984093>

Lock-in Amplifiers  
up to 600 MHz



Watch



# Unveiling carbon dimers and their chains as precursor of graphene growth on Ru(0001)

Min Gao,<sup>1,2,a)</sup> Yan-Fang Zhang,<sup>1,a)</sup> Li Huang,<sup>1</sup> Yi Pan,<sup>1</sup> Yeliang Wang,<sup>1,b)</sup> Feng Ding,<sup>3</sup> Yuan Lin,<sup>2</sup> Shi-Xuan Du,<sup>1,b)</sup> and Hong-Jun Gao<sup>1</sup>

<sup>1</sup>Institute of Physics and University of Chinese Academy of Sciences, Chinese Academy of Sciences, Beijing Key Laboratory for Nanomaterials and Nanodevices, Beijing 100190, China

<sup>2</sup>State Key Laboratory of Electronic Thin Films and Integrated Devices, University of Electronic Science and Technology of China, Chengdu, Sichuan 610054, China

<sup>3</sup>Institute of Textile and Clothing, Hong Kong Polytechnic University, Kowloon, Hong Kong, China

(Received 20 July 2016; accepted 11 September 2016; published online 28 September 2016)

Carbon precursor that forms on the catalyst surface by the dissociation of feedstock gas plays an important role in the controllable growth of graphene on metal substrates. However, the configuration about the precursor has so far remained elusive. Here, we report the direct observation of uniformly structured precursor units and their chain formation at the nucleation stage of graphene growing on Ru(0001) substrate by using scanning tunneling microscopy. Combining this experimental information with density function theory calculations, the atomic-resolved structures of carbon precursor are characterized as adsorbed CH<sub>2</sub> segments on the substrate. The dissociated carbon feedstock molecules or radicals further react to form nonplanar -[C<sub>2</sub>H<sub>4</sub>]- chains adsorbed on hexagonal-close-packed hollow sites of the Ru(0001) substrate before incorporating into the graphene island. These findings reveal that CH<sub>2</sub> and nonplanar -[C<sub>2</sub>H<sub>4</sub>]- segments act as precursors in graphene growth and are helpful to improve the quality and the domain size of desired graphene by precursor or feedstock control. *Published by AIP Publishing.* [<http://dx.doi.org/10.1063/1.4963283>]

Graphene and its modifications exhibit excellent properties and therefore are promising for many important applications, such as lithium batteries,<sup>1–3</sup> supercapacitors,<sup>4,5</sup> thermal management devices,<sup>6</sup> catalysts<sup>7,8</sup> and many other electronics.<sup>9</sup> However, the lack of the technologies for producing high quality graphene in large scale and at low price greatly limits these applications. Nowadays, chemical vapor deposition (CVD) has become a widely used method to synthesize graphene on metal substrate owing to the high efficiency, low cost, and relatively simple apparatus required. Graphene grown on polycrystalline Ni films or copper foil using CVD in ambient environment has been broadly explored. However, the quality is still far from that of mechanically exfoliated graphene.<sup>9,10</sup> Thus, improving the quality and the domain size of CVD graphene is now a great challenge. Understanding the growth process at atomic level is a key issue for achieving such a goal. It is well known that the initial stage in the nucleation process during a chemical reaction is important for the quality of graphene. One of the challenges is the visualization of the initial stage because the nucleation process is too fast to trace directly in experiments. To resolve this problem, the formation process of carbon layer on a single-crystal transition metal surface in a vacuum, investigated several decades ago, re-attracted great attention. Utilizing new and improved techniques, understanding the reaction processes and mechanism of decomposition of hydrocarbons on transition metal surfaces in depth was considered as an effective way to control the formation of graphene. Several groups have conducted theoretical

studies of the initial stage of carbon atoms on different substrates, such as Ir, Ru, Ni, and Cu.<sup>11–15</sup> Some calculation results claimed that carbon atoms prefer to form carbon dimer or linear carbon chains on the substrates at the first stage,<sup>11–14</sup> while Shu *et al.* confirmed that gas-phase decomposition reactions are important integrant of the mechanism of CVD synthesis of graphene.<sup>15</sup> In experiments, some groups tried different methods to detect the initial stage and growth process during the CVD growth of graphene.<sup>16–20</sup> Most experiments only detected the evolution of shape in graphene island during growth.<sup>16–19</sup> McCarty and co-workers proposed that carbon atoms form five-atom clusters on Ru(0001) before attaching to the edge of a graphene island, based on electron reflectivity and theory.<sup>16,21</sup> Niu *et al.* observed different shapes of carbon clusters during the process of graphene formation on Cu(111).<sup>20</sup> Recently, Kirsch *et al.* identified the CCH<sub>2</sub>(ads) during the thermal decomposition of ethylene on Ru surface by high-resolution vibrational spectroscopy.<sup>22</sup> However, rare direct evidence has been observed in experiments. The reaction processes and growth mechanism are still not clear.

*In situ* scanning tunneling microscopy (STM) has been widely used in combination with density functional theory (DFT) calculations to investigate the initial stages of growth processes and chemical reactions.<sup>23</sup> However, it is hard to get the real-space image with atomic structure for the growth process of gas phase on transition metal surface at high temperature by STM. Freezing the initial stage during the growth process is significant to investigate the growth mechanism of graphene by STM. So, it is a requisite to slow down the chemical reaction speed. Nevertheless, it is possible to control the growth process of graphene on a single-crystal transition metal surface in ultrahigh vacuum (UHV) chamber

<sup>a)</sup>M. Gao and Y. Zhang contributed equally to this work.

<sup>b)</sup>Authors to whom correspondence should be addressed. Electronic addresses: ylwang@iphy.ac.cn and sxdu@iphy.ac.cn.

with elaborately controllable amount of reaction gas and temperature.

In the present work, by using *in situ* technique with controllable amount of ethylene and the annealing temperature, we can “freeze” the growth of graphene on Ru(0001) substrate at the initial stage, and then investigate the intermediate states of the growth process. With the help of STM, we find that the carbon atoms form chain structures along the three crystallographic directions of Ru (0001) substrates, e.g., [1000]. Furthermore, DFT calculations reveal that the chain structures are composed of nonplanar  $-\text{[C}_2\text{H}_4\text{]}-$  segments together with  $\text{CH}_2$  segments. Therefore, by combining STM with DFT calculations, we directly observe that  $\text{CH}_2$  and nonplanar  $-\text{[C}_2\text{H}_4\text{]}-$  segments can act as precursors to the growth of epitaxial graphene on Ru(0001), which is a strong evidence to theoretical predictions<sup>11–14</sup> and other indirect experimental results.<sup>22</sup>

Our experiment was conducted in an UHV chamber together with a room temperature STM. The Ru(0001) substrates were cleaned and annealed by a standard process.<sup>24</sup> We exposed the Ru(0001) substrate to ethylene at room temperature and the amount of exposure is 500 L. Then the temperature of the substrate was increased to 1073 K and kept for 10 min. After the temperature of the substrate was decreased to room temperature, it was transported to the STM chamber.

The first-principles calculations were based on DFT and the local density approximation,<sup>25</sup> with the help of the Vienna *ab-initio* simulation package (VASP).<sup>26,27</sup> The projected augmented wave was employed. The kinetic energy cutoff was set to 400 eV. STM images were simulated within the Tersoff–Hamann approximation.<sup>28</sup> Two models were used to represent the Ru(0001) substrate. One is a four-layered slab model ( $5 \times 5$  unit cell) with the two bottom layers fixed, and the other is a two-layered slab model ( $7 \times 7$  unit cell) with the bottom layer fixed. The two-layered slab model is accurate enough for the C-Ru system when local density approximation is used for a large supercell.<sup>29</sup>

The morphology of the Ru(0001) substrate exposed to ethylene at room temperature and annealed to 1073 K was characterized by STM, as shown in Fig. 1. Hydrocarbon gases decompose and form graphene on transition metal substrates, which exhibits moiré patterns because of lattice mismatch.<sup>30</sup> Previous studies have reported the formation of graphene islands on Ru(0001) or Ir(111) substrate when the amount of hydrocarbon gas is not sufficient to form one-layer graphene.<sup>31</sup> In our experiments, graphene islands also formed (marked as dashed lines in Fig. 1(a) and the left part of Fig. 1(b)), and they exhibit high crystal quality of graphene according to the moiré pattern. Besides the well-ordered graphene islands in Fig. 1(b), there are also a large number of isolated bright spots, which exist on the areas of the substrate not covered by graphene. The zoom-in STM images (Figs. 1(b) and 1(c)) further reveal that these bright spots arrange into short chain structures along the three crystallographic directions of Ru(0001) substrates, e.g., [1000]. So these chains have three orientations, induced by the three-fold symmetry of the Ru(0001) substrate. It should be noted that the bright spots have different nearest neighbor distances, as determined from high-resolution STM images in Fig. 1(b). To further understand the structure of the chains, the height profile along

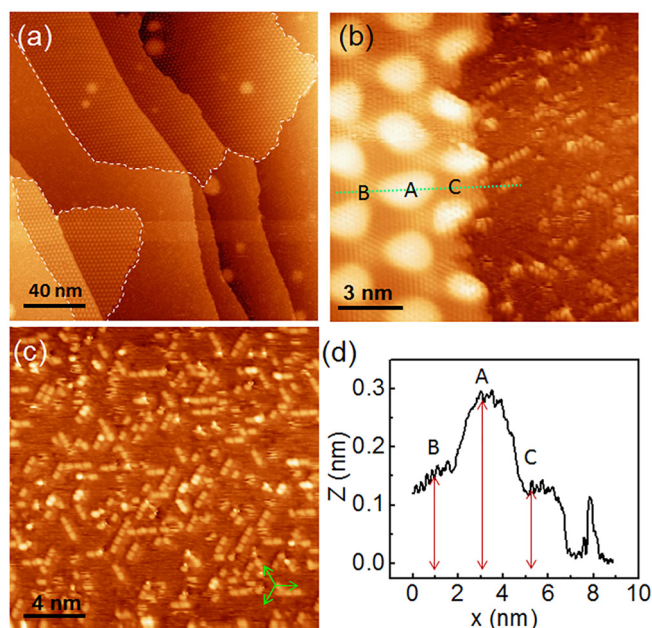


FIG. 1. (a) STM image ( $V_s = -1.1$  V,  $I = 0.18$  nA) of graphene islands on Ru(0001) surface. (b) Atomic resolution STM image ( $V_s = -0.3$  V,  $I = 0.95$  nA) of the edge of graphene islands and the bright spots. The edge of graphene islands is not atomically smooth. (c) STM images ( $V_s = 0.4$  V,  $I = 0.8$  nA) of the chains on Ru(0001). The green arrows indicate three typical directions of these short chains. (d) The height profile along the green line in (b).

the line in Fig. 1(b) is plotted in Fig. 1(d). The height profile shows the corrugation of the graphene and the height of chains simultaneously, which is helpful to analyze the interaction between chains and substrate. Because of the lattice mismatch, graphene on Ru(0001) substrate forms superstructure corrugation, which results in different interaction between carbon atoms and substrate at different corrugation regions. Graphene on Ru(0001) substrate has three different regions, labeled as A, B, and C in Fig. 1(b). Region A is the brightest area and C is the darkest one of graphene in the STM images, signifying the different distances between the graphene and the substrate. It is clearly seen that the height of the bright spots in chains is almost the same as that of carbon atoms near the edge of islands, which is still a little lower than that of the carbon atoms in region C (Fig. 1(d)). This suggests that the carbon atoms in the bright spots have stronger interaction with the Ru(0001) substrate than those graphene does.

The zoom-in STM image (Fig. 2(a)) clearly reveals the orientation and distances among the bright spots in Fig. 1, in which some look like pairs (for example, 1–2, 4–5, 1′–2′, and 3′–4′). Table I summarizes the distances between the nearest-neighbor bright spots in Fig. 2(a). There are two typical distances, 0.26 nm and 0.31 nm. If we consider that the two spots stay closer as a dimer, the chain structures in Fig. 1 are dimer chains with an average dimer-dimer distance of 0.57 nm from STM image. It is well known that the carbon-carbon bond length in free-standing graphene and ethylene are 0.14 and 0.13 nm, respectively. If the dimer chains were composed only of carbon dimers, the bond length of 0.26 nm would be longer than that in graphene and ethylene, implying an unusual weak bond energy in the chains. Even compared with other researchers’ calculated result of carbon

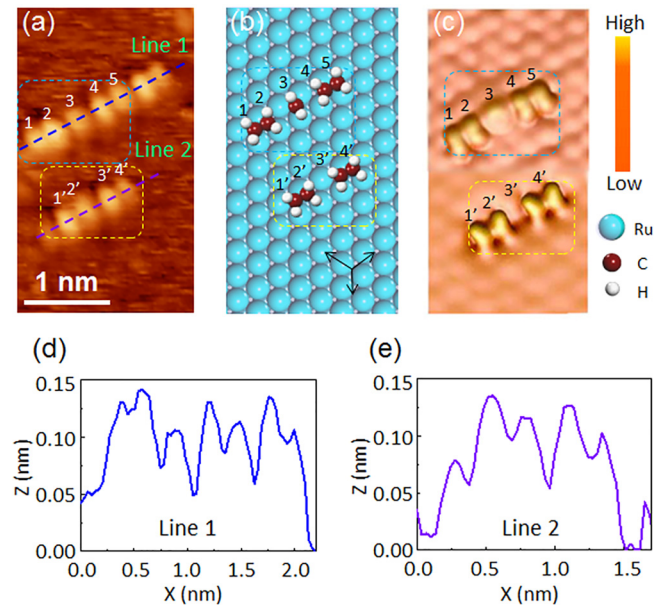


FIG. 2. Carbon precursors observed on Ru(0001). (a) STM image ( $V_S = -0.3$  V,  $I = 0.95$  nA) and (b) possible configurations observed in (a). The black arrows indicate the high-symmetry direction on Ru(0001) surface. (c) STM simulation image according to (b). (d) and (e) are the height profile along the dashed lines 1 and 2 in (a), respectively.

atoms on Ni(111) substrate (0.13 nm), the length is also too long.<sup>11</sup> On the other hand, the fact that the chains are stable at room temperature indicates that the interaction between the chains and the substrate cannot be neglected—it should mainly contribute to the stabilization of the carbon chains. The lattice constant of Ru(0001) substrate is 0.27 nm, which is almost the same as the above length. This relationship implies that Ru(0001) substrate strongly confines the chain structure.

To get a better understanding of the atomic structure of the chains, first-principles calculation was used to investigate the possible configurations of the dimer chains. Since it is reasonable that there is residual hydrogen from the decomposition of ethylene molecules in the UHV system,<sup>16,20,32</sup> several decomposed segments with and without hydrogen, for example, carbon monomers, carbon dimers,  $\text{CH}_2$  and  $\text{C}_2\text{H}_2$ , etc., were tried to figure out what the bright dots are in Fig. 1 (see the details in the [supplementary material](#)). DFT calculation results demonstrate that among all these segments,  $\text{CH}_2$  is the most probable precursor at the initial stage of graphene growth. Figures 2(a)–2(c) present the STM image, the possible geometric structures, and the corresponding STM simulation image of four and five  $\text{CH}_2$  segments on Ru(0001) surface. According to the DFT calculation,  $\text{CH}_2$  prefers to stay at the hexagonal-close-packed (HCP) hollow site of Ru(0001) (see Fig. S1 and Table S1 in the [supplementary material](#)). As a result, the  $\text{CH}_2$  chains stay along the high-symmetry direction of Ru(0001) (Fig. 2(b)), fitting well with

the orientation of the dot chains in STM images (Figs. 1(b) and 2(a)). The distances between the neighboring bright dots both in the STM images and STM simulations are summarized in Table I, showing the distance comparison. The distance between dots 1' and 2' is the same as that between dots 3' and 4', but smaller than that between dots 2' and 3', both in the STM images and in the DFT results. From Table I, the calculation distances between dots 2 and 3, 3 and 4, and 2' and 3' are little smaller than the experimental results. We think that these deviations would come from the experimental errors caused by distortion and drifting of scanning tube, and resolutions of STM images at room temperature, as well as the difference of lattice constant between DFT calculated one the real substrate. So, the difference between experimental distance and the DFT predictions is reasonable. Though the exact value is slightly different, the dimer-like structures are the same in experiment and theoretical prediction. Herein, the STM simulations (Fig. 2(c)) agree well with the experimental results (Fig. 2(a)). In addition, the simulation shows that the bright spots in Fig. 2(c) come from the electron density of hydrogen atoms due to the non-planar configuration of  $\text{CH}_2$  segments. Therefore, the distances between neighboring bright spots in Figs. 2(c) (0.26 nm) and 2(a) (0.26 nm) are actually the distances between the neighboring hydrogen atoms on different carbon atoms, which do not correspond to the C-C bond length in the nonplanar  $\text{C}_2\text{H}_4$  segment. The C-C bond length in the nonplanar  $\text{C}_2\text{H}_4$  segment (0.145 nm) is very close to that in graphene (0.141 nm). In conclusion, our calculations, along with their agreement with the experimental observations, indicate that  $\text{CH}_2$  and nonplanar  $\text{C}_2\text{H}_4$  segments are the precursors at the initial stage of graphene growth.

The initial stage of carbon atoms is critical to the growth of graphene on metal substrate, which particularly affects the nucleation and shape of graphene. Previously, Luo *et al.* reported that the graphene island is shaped like a flower when the attachment to the island is carbon clusters.<sup>33</sup> They also found that when individual carbon atoms attach to the edge of graphene islands, the graphene islands are triangular in shape, and the edge of islands is atomically smooth. Here, we can see that the shape of the graphene islands in Fig. 1(a) is almost triangular, but with an edge that is not so smooth. Moreover, the atomic resolution STM image of the edge of graphene islands, shown in Fig. 1(b), demonstrates that the edge of the island is not atomically smooth, although the direction is almost along the zig-zag line of graphene. And we also see that the  $\text{CH}_2$  segments form  $\text{C}_2\text{H}_4$  dimer or  $-\text{[C}_2\text{H}_4\text{]}-$  chains near the edge of the graphene. The irregular shape of graphene islands and the existence of  $\text{CH}_2$  segments around the graphene islands in our results further confirm that the  $\text{CH}_2$  segments are precursors during the growth of epitaxial graphene.

To further investigate the chemical activity of carbon chains, we exposed the sample to oxygen at 873 K. The pressure of oxygen was  $5 \times 10^{-7}$  mbar and the duration was 30 s. Afterward, we can observe two changes of the sample by STM, as shown in Figs. 3(a) and 3(b). One change is that the surface of the substrate not covered by graphene becomes clean, demonstrating that the carbon chains disappear. The other is that the shape of the graphene islands becomes more regular. From the high resolution STM image in Fig. 3(c),

TABLE I. Distances between neighboring dots in Fig. 2.

	$d_{12}$	$d_{23}$	$d_{34}$	$d_{45}$	$d_{1'2'}$	$d_{2'3'}$	$d_{3'4'}$
Exp. (nm)	0.26	0.31	0.31	0.26	0.26	0.31	0.26
DFT (nm)	0.26	0.29	0.29	0.26	0.26	0.29	0.26

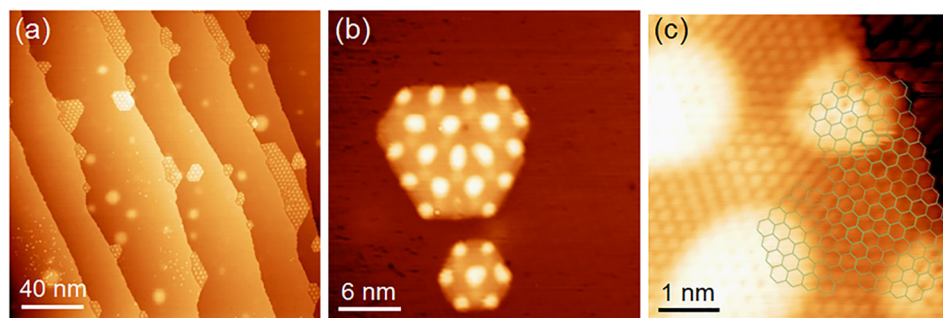


FIG. 3. STM images of graphene islands after the exposure of the sample to oxygen. (a)  $200\text{ nm} \times 200\text{ nm}$  ( $V_s = -1.5\text{ V}$ ,  $I = 0.1\text{ nA}$ ). (b)  $60\text{ nm} \times 60\text{ nm}$  ( $V_s = -1\text{ V}$ ,  $I = 0.14\text{ nA}$ ). (c) Atomic resolution STM image ( $V_s = -0.12\text{ V}$ ,  $I = 1.42\text{ nA}$ ) of the smooth edge of graphene islands on Ru(0001).

we see that the edges of the islands are zigzag and atomically smooth, the same as those etched by plasma.<sup>34</sup> These results show that the  $\text{CH}_2$  segments in dimer chains are as active as those at the edge of graphene islands and can be oxidized more easily. The oxygen etching results indicate that the  $\text{CH}_2$  segments in the chains are easily oxidized.

In summary, by controlling the exposure amount of hydrocarbon and the annealing temperature, we directly observed  $\text{CH}_2$  and  $-\text{[C}_2\text{H}_4\text{]-}$  chains as precursors for graphene grown on Ru(0001) substrate. Combining the experiments with theoretical calculations, the atomic structures and the preferred adsorption sites on the Ru(0001) surface are fully revealed. It is further confirmed that the decomposed feedstock molecules first form  $\text{CH}_2$  radicals adsorbed on the HCP hollow sites of the Ru(0001) surface. The absorption interaction of the  $\text{CH}_2$  segments further leads to the nonplanar  $-\text{[C}_2\text{H}_4\text{]-}$  chains as the precursors of graphene grown on the Ru(0001) surface. Our study has revealed the feedstock transition states of graphene grown on Ru(0001) surface and therefore is vital for the understanding of graphene's growth mechanism and further improvement of the experimental technology for desired graphene growth.

Clusters of C,  $\text{C}_2$ , and  $\text{C}_2\text{H}_2$  adsorbed on Ru(0001) and  $\text{CH}_2$  on different adsorption sites on Ru(0001) can be found in supporting information.

See [supplementary material](#) for the possible precursors, the adsorption sites and the distances between neighbors. The distances between neighboring C,  $\text{C}_2$ , and  $\text{C}_2\text{H}_2$  in these configurations don't agree with the experiment data except for  $\text{CH}_2$ . The most stable adsorption site for  $\text{CH}_2$  adsorbed on a Ru(0001) surface is HCP hollow.

We thank Professor Sokrates T. Pantelides and Dr. Yuyang Zhang for helpful discussions. We acknowledge the financial support from National Key Research & Development Projects of China (2016YFA0202300), the National Basic Research Program of China (2013CBA01600), the National Natural Science Foundation of China (Nos. 51325204, 61390501, 61222112, 51572290, and 61306015), the Chinese Academy of Sciences (Nos. 1731300500015 and XDB07030100), and the National Supercomputing Center in Tianjin.

<sup>1</sup>B. Z. Jang, C. G. Liu, D. Neff, Z. N. Yu, M. C. Wang, W. Xiong, and A. Zhamu, *Nano Lett.* **11**(9), 3785 (2011).

<sup>2</sup>X. Zhao, C. M. Hayner, M. C. Kung, and H. H. Kung, *Adv. Energy Mater.* **1**(6), 1079 (2011).

<sup>3</sup>Y. X. Yu, *Phys. Chem. Chem. Phys.* **15**(39), 16819 (2013).

<sup>4</sup>C. G. Liu, Z. N. Yu, D. Neff, A. Zhamu, and B. Z. Jang, *Nano Lett.* **10**(12), 4863 (2010).

<sup>5</sup>Y. Zhu, S. Murali, M. D. Stoller, K. J. Ganesh, W. Cai, P. J. Ferreira, A. Pirkle, R. M. Wallace, K. A. Cychosz, M. Thommes, D. Su, E. A. Stach, and R. S. Ruoff, *Science* **332**(6037), 1537 (2011).

<sup>6</sup>Z. Yan, G. Liu, J. M. Khan, and A. A. Balandin, *Nat. Commun.* **3**, 827 (2012).

<sup>7</sup>R. L. Liu, D. Q. Wu, X. L. Feng, and K. Mullen, *Angew. Chem., Int. Ed.* **49**(14), 2565 (2010).

<sup>8</sup>R. Gholizadeh and Y. X. Yu, *Appl. Surf. Sci.* **357**, 1187 (2015).

<sup>9</sup>K. S. Kim, Y. Zhao, H. Jang, S. Y. Lee, J. M. Kim, K. S. Kim, J.-H. Ahn, P. Kim, J.-Y. Choi, and B. H. Hong, *Nature* **457**(7230), 706 (2009).

<sup>10</sup>X. S. Li, W. W. Cai, J. H. An, S. Kim, J. Nah, D. X. Yang, R. Piner, A. Velamakanni, I. Jung, E. Tutuc, S. K. Banerjee, L. Colombo, and R. S. Ruoff, *Science* **324**(5932), 1312 (2009).

<sup>11</sup>J. F. Gao, Q. H. Yuan, H. Hu, J. J. Zhao, and F. Ding, *J. Phys. Chem. C* **115**(36), 17695 (2011).

<sup>12</sup>H. Chen, W. G. Zhu, and Z. Y. Zhang, *Phys. Rev. Lett.* **104**(18), 186101 (2010).

<sup>13</sup>Y. Li, M. Li, T. Wang, F. Bai, and Y.-X. Yu, *Phys. Chem. Chem. Phys.* **16**(11), 5213 (2014).

<sup>14</sup>A. Harpale, M. Panesi, and H. B. Chew, *J. Chem. Phys.* **142**(6), 061101 (2015).

<sup>15</sup>H. Shu, X.-M. Tao, and F. Ding, *Nanoscale* **7**(5), 1627 (2015).

<sup>16</sup>E. Loginova, N. C. Bartelt, P. J. Feibelman, and K. F. McCarty, *New J. Phys.* **11**, 063046 (2009).

<sup>17</sup>Z.-J. Wang, G. Weinberg, Q. Zhang, T. Lunkenbein, A. Klein-Hoffmann, M. Kurnatowska, M. Plodinec, Q. Li, L. Chi, R. Schloegl, and M.-G. Willinger, *ACS Nano* **9**(2), 1506 (2015).

<sup>18</sup>P. R. Kidambi, B. C. Bayer, R. Blume, Z.-J. Wang, C. Baetz, R. S. Weatherup, M.-G. Willinger, R. Schloegl, and S. Hofmann, *Nano Lett.* **13**(10), 4769 (2013).

<sup>19</sup>P. C. Rogge, S. Nie, K. F. McCarty, N. C. Bartelt, and O. D. Dubon, *Nano Lett.* **15**(1), 170 (2015).

<sup>20</sup>T. Niu, M. Zhou, J. Zhang, Y. Feng, and W. Chen, *J. Am. Chem. Soc.* **135**(22), 8409 (2013).

<sup>21</sup>E. Loginova, N. C. Bartelt, P. J. Feibelman, and K. F. McCarty, *New J. Phys.* **10**, 093026 (2008).

<sup>22</sup>H. Kirsch, Y. J. Tong, and R. K. Campen, *ChemCatChem* **8**(4), 728 (2016).

<sup>23</sup>H. Zhou, J. Liu, S. Du, L. Zhang, G. Li, Y. Zhang, B. Z. Tang, and H.-J. Gao, *J. Am. Chem. Soc.* **136**(15), 5567 (2014).

<sup>24</sup>M. Gao, Y. Pan, C. D. Zhang, H. Hu, R. Yang, H. L. Lu, J. M. Cai, S. X. Du, F. Liu, and H. J. Gao, *Appl. Phys. Lett.* **96**(5), 053109 (2010).

<sup>25</sup>P. E. Blöchl, *Phys. Rev. B* **50**(24), 17953 (1994).

<sup>26</sup>G. Kresse and J. Hafner, *Phys. Rev. B* **47**(1), 558 (1993).

<sup>27</sup>G. Kresse and J. Furthmüller, *Comput. Mater. Sci.* **6**(1), 15 (1996).

<sup>28</sup>J. Tersoff and D. R. Hamann, *Phys. Rev. B* **31**(2), 805 (1985).

<sup>29</sup>L. Z. Zhang, S. X. Du, J. T. Sun, L. Huang, L. Meng, W. Y. Xu, L. D. Pan, Y. Pan, Y. L. Wang, W. A. Hofer, and H. J. Gao, *Adv. Mater. Interfaces* **1**(3), 1300104 (2014).

<sup>30</sup>S. Marchini, S. Gunther, and J. Winterlin, *Phys. Rev. B* **76**(7), 9 (2007).

<sup>31</sup>P. W. Suiter, J. I. Flége, and E. A. S. Er, *Nat. Mater.* **7**(5), 406 (2008).

<sup>32</sup>W. Zhang, P. Wu, Z. Li, and J. Yang, *J. Phys. Chem. C* **115**(36), 17782 (2011).

<sup>33</sup>Z. T. Luo, S. Kim, N. Kawamoto, A. M. Rappe, and A. T. C. Johnson, *ACS Nano* **5**(11), 9154 (2011).

<sup>34</sup>Z. W. Shi, R. Yang, L. C. Zhang, Y. Wang, D. H. Liu, D. X. Shi, E. G. Wang, and G. Y. Zhang, *Adv. Mater.* **23**(27), 3061 (2011).